Food Chemistry: X 17 (2023) 100573

Contents lists available at ScienceDirect

Food Chemistry: X

journal homepage: www.sciencedirect.com/journal/food-chemistry-x

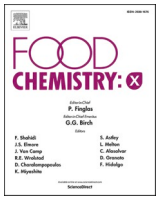

High oxygen-modified packaging (HiOx-MAP) mediates HIF-1α regulation of tenderness changes during postmortem aging of yak meat

Ke-qi Xin, Kai Tian, Qun-li Yu *, Ling Han *

College of Food Science and Engineering, Gansu Agricultural University, Lanzhou, China

ARTICLE INFO

Keywords:
Tenderization
Apoptosis
High-oxygen packaging
Yak

ABSTRACT

In the present study, we studied the effect of high oxygen-modified packaging (HiOx-MAP) on yak meat tenderness and the underlying mechanism. HiOx-MAP significantly increased the myofibril fragmentation index (MFI) of yak meat. In addition, western blotting showed that the expression of hypoxia-inducible factor (HIF-1α) and ryanodine receptors (RyR) in the HiOx-MAP group was reduced. HiOx-MAP increased the activity of sarcoplasmic reticulum calcium-ATPase (SERCA). The energy disperse spectroscopy (EDS) mapping showed gradually reduced calcium distribution in the treated endoplasmic reticulum. Furthermore, HiOx-MAP treatment increased the caspase-3 activity and the apoptosis rate. The activity of calmodulin protein (CaMKKβ) and AMP-activated protein kinase (AMPK) was down-regulated leading to apoptosis. These results indicated that HiOx-MAP promoted apoptosis during postmortem aging to improve the tenderization of meat.

1. Introduction

The tenderness of the meat is a trait that decides its purchase by consumers and determines its edible quality (Hopkins, 2017). For example, poor tenderness is one of the major factors that contributes to a decline in the quality of plateau yak meat (> 3500) with hypoxia, resulting in substantial obstacles to the development of the yak meat and meat industry. Therefore, it is highly essential to investigate the underlying mechanism of yak meat tenderness. Hypoxia enhances the rate of glycolysis and inhibits mitochondrial oxygen consumption in yak meat during postmortem aging (Xin et al., 2022). Thus, hypoxia induces the glycolysis pathway of meat, and the downregulation of pH contributes to worse tenderness (Wicks et al., 2019). Furthermore, apoptotic enzymes and caspases—proteolytic enzymes involved in protein degradation, are activated to cause the degradation of myofibrils during postmortem hypoxia (Chen et al., 2015). These findings indicate that the oxygen concentration of meat during postmortem aging is related to tenderness.

The conversion of muscle to meat is a complex process involving several biochemical and metabolic reactions. Especially, the apoptotic pathway plays a significant role in the tenderization of meat (Hopkins, 2017). We have previously reported that the differences in yak meat tenderness at different altitudes were significantly related to hypoxia-inducible factor-1α (HIF-1α) (Xin et al., 2022). Interestingly, hypoxia is related to apoptosis, the degree of which determines whether cells undergo apoptosis or survive by adapting to hypoxia (Greijer, & Van, 2004). HIF-1α is a known key hypoxia-activated transcription factor that regulates metabolic adaptation, metastasis, and anti-apoptosis of hypoxic cells. In addition, a study reported that acquired anti-apoptosis under hypoxic conditions is related to the upregulation of the inhibitor of apoptosis protein-2 (Dong et al., 2001). Under hypoxic conditions, high levels of glucose transporter-1 (GLUT-1) inhibit apoptosis in an extracellular glucose concentration-independent manner by inhibiting stress-activated protein kinase activation. Consequently, HIF-1α resists the apoptosis of hypoxic cells by increasing the expression of GLUT-1 (Kilic et al., 2007). Moreover, the physiological state of animals before slaughter greatly affects the meat quality. Poor quality of meat is often accompanied by excessive glucocorticoid (GC) release (Yoshioka et al., 2005). In addition, GC can induce apoptosis in several cell lines in a calcium ion-dependent manner. Calcium-activated neutral proteolytic enzyme inhibitors inhibit GC-induced apoptosis. In addition, elevated levels of intracellular free calcium have been detected during HIF-1-induced apoptosis (Khan et al., 1996). Calcium/calmodulin-dependent kinases (CaMKs) are important calcium-modulating proteins, of which calmodulin protein (CaMKK) is the only AMP-activated protein kinase (AMPK) upstream kinase regulated by Ca^{2+} release during muscle contraction. When sarcoplasmic Ca^{2+} levels are elevated, the activity of CaMKKβ is increased through the Ca^{2+}/calmodulin complex (Tokumitsu

* Corresponding authors.
E-mail address: yuqunligsau@163.com (L. Han).

https://doi.org/10.1016/j.fochx.2023.100573
Received 28 September 2022; Received in revised form 3 January 2023; Accepted 6 January 2023
Available online 9 January 2023

et al., 2001). Moreover, CaMKK is activated to regulate ATP/AMP to maintain a dynamic balance, and CaMKKβ can phosphorylate AMPK Thr172 site to activate AMPK (Morales-Alamo et al., 2012). AMPK primarily completes the uptake and transport of glucose by promoting the transfer of GLUT1 to the cell membrane and phosphorylating the transcription factors to induce the expression of the *GLUT-1* gene (Winder, & Hardie, 1999). We have previously confirmed that HIF-1α is positively correlated with GLUT-1 expression during postmortem yak maturation and its expression significantly increases and then decreases with aging time (Xin et al., 2022). Laver (2018) found that HIF-1α-mediated sarcoplasmic reticulum pressure instability releases calcium from the endoplasmic reticulum, whereas its dysfunction induces apoptosis (Luciani et al., 2009). In addition to catalyzing glycolysis, hexokinase is involved in regulating the translocation of the mitochondrial membrane after binding to voltage-dependent anion channels (VDAC) to negatively regulate the cleavage of Bid, activate pro-apoptotic molecules Bax and Bak, and possibly direct the inhibition of Bad, thus preventing the release of cytochrome *c* into the cytoplasm and consequently arresting apoptosis (Fulda, & Debatin, 2007). However, it remains unclear whether muscle cell apoptosis and meat tenderness are initiated through the HIF-1α-calcium signaling and warrants further research.

High oxygen-modified packaging (HiOx-MAP) is employed for preserving the fresh beef color, HiOx-MAP (80 % O_2/20 % CO_2) has been shown to effectively enhance the quality of meat by increasing its lightness and redness values and surface color (Lu et al., 2020). Because 50 % O_2 can result in a normal pH, with a beef color similar to that under 80 % O_2 storage d (Yang et al., 2021), the effect on meat color under a regular 80 % O_2-HiOx-MAP package is positive. Moreover, the literature reports no study on the effect of change in O_2 concentration on beef tenderness. Therefore, we studied the comprehensive effect of oxygen levels on yak meat and methods to improve its tenderness.

2. Materials and methods

2.1. Meat samples

The longissimus thoracis et lumborum (LTL) were given at a local abattoir from five domestic yaks (*Bos grunniens*; altitude: 4500 m; 3.5 years; 200 kg). The protocol and procedures followed were in accordance with the approved guidelines of the Institutional Animal Care and Use Committee of Gansu Agricultural University (approved ID: 2012-2-159). Yak meat was obtained from the carcasses within 0.5 h and cut into 3 cm sections after connective tissue and obvious fat were removed to vacuum packaged (DT-6D packaging machine, Chengdu Tongheng Packaging Co., ltd., Chengdu, China). In total, 100 g of each meat sample was packaged in 80 %O_2-MAP (80 % O_2 + 20 % CO_2), 50 %O_2-MAP (50 % O_2 + 50 % CO_2), and 0 %O_2-MAP (vacuum packaging) and stored at 4 °C. In total, five yak meat samples were collected for each treatment with five replicates in all treatments (w = 5). Meat samples were packaged using polypropylene trays (Model TQBC-0775, Sealed Air Packaging Co., ltd., Shanghai, China), absorbent pads (Cryovac Dri-Loc® AC-50, Sealed Air Packaging Co., ltd., Shanghai, China), and oxygen-barrier films (Lid 1050, Sealed Air Packaging Co., ltd., Shanghai, China). Packaged samples were stored at 4 °C for 0, 12, 24, 48, and 120 h, following which the indicators indicating that samples cannot be frozen were immediately measured, whereas other samples were stored at −80 °C until measured.

2.2. Oxygen consumption (OC) and oxygen penetration depth (OPD)

Oxygen consumption was determined by quantifying the deoxidation of Mb in a ratio of K/S474 and K/S525 (AMSA, 2012). The ratio of K/S474 and K/S 525 is inversely proportional to OC. Next, the ratio was converted using the formula [1.5-(K/S474 ÷ K/S 525)] to obtain a big OC value (AMSA, 2012). Afterward, the converted values were converted to percentages for easier visualization; to convert ratios to relative percentages, the highest numerical OC ratio was considered to be 100 %, whereas other treatment combinations were calculated relative to the highest OC ratio (Yang et al., 2022).

Oxygen penetration depth was calculated according to the method described by Lu et al. (2020) with a few modifications. A vertical section perpendicular to the surface of the yak sample was used to observe a subsurface cross-section. The OPD value was detected in millimeters by a digital caliper. The average of the three results was taken in each meat sample.

2.3. Western blotting

The yak meat samples (60 mg) were homogenized in 200 μL of RIPA lysis buffer containing 1 mM PMSF protease inhibitor. The homogenates were centrifuged at 10,010 g for 10 min at 4 °C. The total protein content of the supernatant was detected using the BCA kit (Beyotime, Shanghai, China) and the expression of the target protein was detected. The total protein samples were boiled and then protein loading buffer (4:1) for 15 min. The proteins were separated using 30 % (29.1) SDS-PAGE separation and 5 % stacking gels (in a wet transfer apparatus. Protein bands were transferred to PVDF membranes (Bio-Rad Laboratories, California, USA). The membranes were placed in a mixture containing skimmed milk powder (5 %), Tween (TBST: 10 mM Tris + 0.1 % Tween-20 + 150 mM NaCl), and Tris-buffered saline, and subsequently incubated with the following antibodies: 1:2,000 dilution GAPDH mouse monoclonal (Abcam, Cambridge, UK); HIF-1α polyclonal rabbit anti-mouse (Abcam, Cambridge, UK); 1:1,000 RyR polyclonal rabbit anti-mouse (Abcam, Cambridge, UK) at 4 °C. Next, TBST was used for washing, and goat anti-rabbit (Abcam, Cambridge, UK) secondary antibodies (dilution 1:3,000) were added for 1 h and the membranes were washed again. Finally, the enhanced chemiluminescence reagent was added and membranes were stained for 15 s before being thoroughly washed with water. The visualizing protein blots were measured by an E-gel imaging system and the ImageJ software (Thermo, Beijing, China; National Institutes of Health) was used for analysis.

2.4. Preparation of endoplasmic reticulum, isolation of mitochondria and detection of Ca^{2+} concentration

Measurements were performed according to the method of Li et al. (1999). Briefly, 5 g of meat samples were chopped and added into buffer A (70 mmol sucrose, 2.0 mmol EDTA, 5.0 mmol 4-morph propanoic acid, 220 mmol mannitol, 0.5 % bovine serum albumin (BSA) according to the 1:10 homogenate. After centrifugation at 1000 g at 4 °C for 10 min, the supernatant was centrifuged at 8000 g/min at 4 °C for 20 min. The final supernatant was suspended in buffer B (buffer A without BSA was diluted 7.5 times, pH 7.4).

The endoplasmic reticulum was extracted according to the methods described by MacLennan (1970) with little modification. Briefly, 2 g of meat sample and 10 mL extraction buffer (0.25 mol/L sucrose, 10 mmol/L Tris, pH = 7.4) were added to the homogenate at 4 °C for 30 s. The homogenate was centrifuged at 4 °C for 2000 r/min for 10 min and then centrifuged at 10,000 r/min for 15 min. The supernatant was centrifuged at 22,000 r/min at 4 °C for 50 min, and the precipitation obtained contained the sarcoplasmic reticulum. The precipitate was re-suspended in buffer (0.25 mol/L sucrose, 10 mmol/L Tris-HCL, pH = 8.0.

The Ca^{2+} concentration was detected by the method described by Zhang et al. (2018) using certain modifications with an Ion 450 Ion radiator analyzer connected by a REF201 reference calomel electrode and an ISE25Ca calcium selective electrode (HACH, Loveland, America). Next, a 10 mL suspension was centrifuged at 4 °C for 20 min at 20,000 g, and the supernatant (4 mL) was mixed with 80 μ/L 4 mL/L KCL for testing. A calibration curve was obtained before each sample to create the relationship between mV and concentration. All samples were processed at 20 ± 1 °C, and each measurement was performed using the

standard addition method.

2.5. Determination of membrane permeability transition pore (MPTP) opening and the depolar-ization of mitochondrial membrane potential ($\Delta\Psi m$)

The MPTP opening was analyzed using the method described by Wang et al. (2018). Briefly, 3.0 mL of MPTP coolant (70 mmol sucrose, 230 mmol mannitol, pH = 7.4, 3.0 mmol HEPES) was added to mitochondrial suspension until the concentration reached to 0.3 mg/mL. Afterward, 3.0 mL cooled solution was mixed with mitochondrial particle solution (1.0 mL) and the absorbance value (540 nm) by the Shimadzu Corporation UV2550 spectrometer in Japan.

Using a JC-1 Assay Kit (Beyotime, Beijing, China) to detect the ΔΨm value. Mitochondrial pellets (0.1 mL) were incubated in 0.9 mL of JC-1 dying working solution and mortar at 4 °C for 20 min. The monomeric fluorescence intensity and aggregated forms of JC-1 were achieved using a fluorescence spectrophotometer, respectively, testing the absorbance at 525/590 nm and 490/530 (emission/excitation) (Shimadzu RF 5301, Kyoto, Japan).

2.6. Determination of enzyme activity

The activity of CaMKKβ, AMPK, and SERCA was performed using a standard commercial kit from Blue Gene Biotechnology Co., ltd. (Shanghai, China). Briefly, 0.6 g of meat samples were obtained and placed into a pre-cooled centrifuge tube. Frozen homogenate ice bath homogenate (6000 r/min) was added at the rate of 1:5 (m/V). The supernatant was centrifuged at 12.000 r/min at 4 °C for 6 min. The optical density (OD) at 450 nm was measured using an enzyme-linked immunosorbent assay (ELISA) and a calibration curve was obtained based on the OD values corresponding to each of the standard concentrations (Shen et al., 2014).

The activity of Caspase-9 and Caspase-3 was determined using the method described by Wang et al. (2018). Briefly, 90 mg of meat samples were chopped and added to 150 μL of a cracking buffer, and then homogenized and centrifuged for 10 min (12,000 rpm, 4 °C). This culture supernatant was incubated at caspase analysis buffer with DEVD-*p*NA at 37 °C for 2 h and the absorbance was measured at 405 nm by a micro tablet (Thermo Science, USA). Finally, the activity of caspase-9 and caspase-3 was assessed using the caspase activity colorimetric assay kit (Pulitzer, Beijing, China).

The proline hydroxylase domain (PHD) activity was determined by referring to Kaluz et al. (2021), 1 g of meat sample was weighed and cut into pieces, and 9 mL of PBS buffer was added and centrifuged at 4 °C at 6000 g for 10 min. The PHD activity kit was used to detect PHD enzyme activity in the supernatant. The number of PHD activity units (U) per g of muscle tissue indicates the PHD activity.

Table 1
Effects of oxygen concentrations and aging time on the oxygen consumption (OC) and oxygen penetration depth (OPD) of yak during postmortem aging.

Parameters	Packaging	Aging time (h)				
		0	6	12	24	120
OC (%)	0 %O_2	97.76 ± 0.22^{a}	95.39 ± 0.26^{Ab}	90.76 ± 0.56^{Ac}	89.49 ± 0.28^{Ad}	76.06 ± 0.25^{Ae}
	50 %O_2 + 50 %CO_2	97.76 ± 0.22^{a}	92.15 ± 0.08^{Bb}	89.14 ± 0.12^{Bc}	85.91 ± 0.06^{Bd}	75.54 ± 0.29^{Be}
	80 %O_2 + 20 %CO_2	97.76 ± 0.22^{a}	90.22 ± 0.32^{Cb}	87.32 ± 0.20^{Cc}	85.41 ± 0.07^{Bd}	75.27 ± 0.59^{Be}
OPD (nm)	0 %O_2	1.06 ± 0.01^{c}	1.07 ± 0.01^{Cb}	1.07 ± 0.01^{Cb}	1.08 ± 0.01^{Ca}	1.08 ± 0.01^{Ca}
	50 %O_2 + 50 %CO_2	1.06 ± 0.01^{e}	5.27 ± 0.01^{Bd}	5.49 ± 0.01^{Bc}	5.87 ± 0.02^{Bb}	6.65 ± 0.02^{Ba}
	80 %O_2 + 20 %CO_2	1.06 ± 0.01^{e}	6.33 ± 0.02^{Ab}	6.48 ± 0.05^{Ac}	6.77 ± 0.02^{Ab}	6.96 ± 0.02^{Aa}

2.7. Fluorescence double staining

Meat samples were confirmed with polyclonal rabbit anti-mouse, 1:1000, (Abcam, Cambridge, UK) according to the method described by Chen et al. (2010) with slight modifications. The muscle blocks were sliced using a CM1850 microtome (Leica Biosystems, Germany) at −25 °C and sections on a glass slide. Frozen muscle sections were air-dried with a fan and incubated with the mixed solution (1 % Triton X-100, 0.5 % BSA in PBS) for 30 min, followed by incubation with antibodies against CaMKKβ (mouse monoclonal; Abcam, Cambridge, UK) and AMPK (anti-mouse; Abcam). Afterward, the slides were rinsed again with PBS and incubated with secondary antibodies (goat anti-rabbit, 1:3000) for 1 h. Finally, the sections were washed in PBS and deionized water, and next fixed with an aqueous fixation medium. The histochemical section was observed with a bright field microscope, and the immunohistochemical fluorescence image was observed using the EVOS FL automatic imaging system (Life Technologies). The fluorescence microscope was equipped with FITC filters (470–510 nm) and a 20 × objective lens was used to acquire images from each muscle section.

Note: BSA: bovine serum albumin; PBS: phosphate buffered solution.

2.8. Myofibril fragmentation index (MFI)

The MFI was measured using the method described by Wang et al. (2018) with small modifications. Briefly, 2.0 g of meat was minced and mixed in (20 mM K_3PO_4, 1 mM NaN_3, 100 mM KCl; 1 mM EDTA, 1 mM $MgCl_2$, pH 7.1) buffer solution. The mixed samples were first homogenized for 30 s (10,000 rpm; 4 °C) and centrifuged at 1,000 rpm for 20 min. The precipitate was suspended in buffer (8 volumes), centrifuged, and using a mesh screen (200) to filter the precipitate containing 10 volumes of buffers. The absorbance (540 nm) value was recorded by the UV2550 ultraviolet spectrophotometer from Japan Shimadzu Corporation. The final result of the MFI was obtained by multiplying the reading by 200.

2.9. EDS mapping

The Ca^{2+} distribution of mitochondria and sarcoplasmic reticulum were analyzed by environmental scanning electron microscopy with Energy Dispersive X-ray Spectroscopy (ESEM-EDS) during postmortem aging. The Ca^{2+} distribution was measured using the method described by López-Arce et al. (2011) with small modifications. The sample was fixed on a temperature-controlled sample cup, and the temperature was controlled at −25 °C through the cold stage to cool and solidify the samples. The surface element distributions of samples were investigated by scanning electron microscopy (SEM, 40 kV acceleration voltage, S-4300, Hitachi) using EDS mapping under an accelerating voltage of 15 kV.

2.10. TdT-mediated dUTP nick-end labeling (TUNEL)

The apoptosis of nuclei was determined using the TdT-mediated dUTP nick-end labeling (TUNEL) Assay Kit according to the manufacturer's instructions (Key Gen, Nanjing, China). First, the sample was cut into thin paraffin sections (5 μm) before these were dewaxed and sealed with 3 % H_2O_2 and methanol (100 %) for around 10 min at room temperature. The proteolytic enzyme K (100 μL) was mixed for 30 min and placed in TdT (50 μL) for incubation for 1 h at 37 °C; subsequently, streptavidin-fluorescein labeled buffer was added and incubated in darkness for 30 min. The anti-FITC solution was coupled with 50 μL of POD in darkness (37 °C, 30 min), and afterward, DAB was mixed into a color rendering. The positive nuclei were added with 50 U/μL deoxyribonuclease I for 30 min, followed by addition of the TUNEL reaction

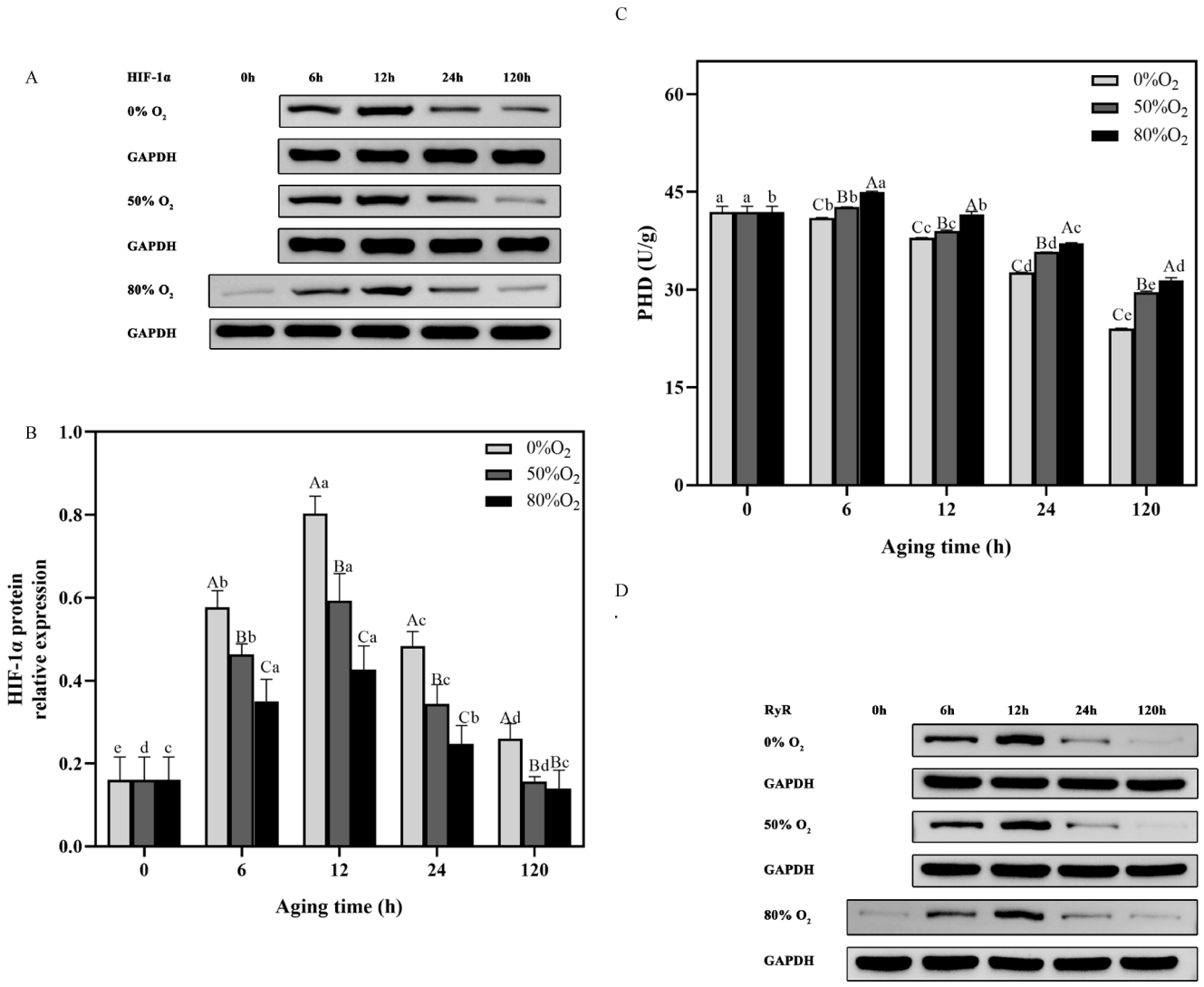

Fig. 1. (A/B) Representative Western blots of HIF-1α in 0 % O_2-HiOx-MAP, 50 % O_2-HiOx-MAP and 80 % O_2-HiOx-MAP groups. GAPDH was used as loading control (A/B). Relative values were calculated as the intensity of the HIF-1α band over that at 0 h. HIF-1α levels of yak meat in the three groups stored at 4 °C for 0, 6, 12, 24, and 120 h as shown. (C) The activity of proline hydroxylases (PHD) in 0 % O_2-HiOx-MAP, 50 % O_2-HiOx-MAP and 80 % O_2-HiOx-MAP groups. The activity of PHD in yak meat in the three groups stored at 4 °C for 0, 6, 12, 24, and 120 h as shown. (D/E) Representative Western blots of ryanodine receptors (RyR) in 0 % O_2-HiOx-MAP, 50 % O_2-HiOx-MAP and 80 % O_2-HiOx-MAP groups. GAPDH was used as loading control (D/E). RyR levels of yak meat in the three groups stored at 4 °C for 0, 6, 12, 24, and 120 h as shown. (F) The activity of sarcoplasmic reticulum calcium-ATPase (SERCA) in 0 % O_2-HiOx-MAP, 50 % O_2-HiOx-MAP and 80 % O_2-HiOx-MAP groups. The activity of SERCA in yak meat in the three groups stored at 4 °C for 0, 6, 12, 24, and 120 h as shown. (G) The distribution of sarcoplasmic reticulum calcium in 0 % O_2-HiOx-MAP, 50 % O_2-HiOx-MAP and 80 % O_2-HiOx-MAP groups and green fluorescence expressed Ca^{2+}.Note: The capital letters represent the difference of all treatment groups and the lowercase letters represent stands the difference of the postmortem aging ($P < 0.05$). Error bars indicate the standard errors of the mean.

mixture. All treatments were assessed under a CKX31 fluorescence microscope (Olympus, Japan), and the apoptosis rate was calculated using the number of positive nuclei in all sample section.

2.11. Statistical analysis

Statistical analysis was performed using Statistical Product and Service Solutions (SPSS) (version 19.0, Chicago, IL, USA). Each result is expressed as means of three results and expressed as mean ± standard error (SE). All data were analyzed using the one-way analysis of variance (ANOVA) combined with Duncan's new multiple-range test ($P < 0.05$).

3. Results and discussion

3.1. Determination of oxygen consumption and oxygen penetration depth from yak meat

We found that changes in oxygen solubility affected the relationship between yak meat and oxygen consumption in different packaging types of yak meat samples during aging. Table 1 shows the changes in oxygen consumption of yak with different packaging types during postmortem aging. The oxygen consumption resulted in a significant decrease with aging time, showing that the oxygen demand reduced with increasing postmortem time ($P < 0.05$). Moreover, the oxygen consumption value of 80 % O_2-HiOx-MAP packaging was significantly lower than ($P < 0.05$) that of 50 % O_2-HiOx-MAP packaging from 0 h to 12 h; however, it became insignificant from 24 h to 120 h. This result indicated that the

E

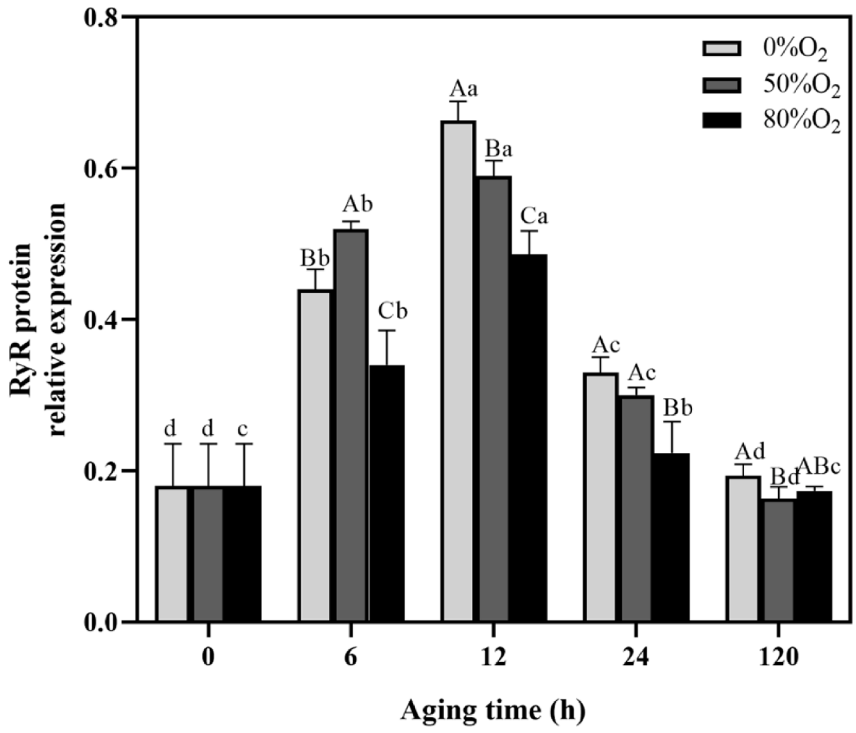

F

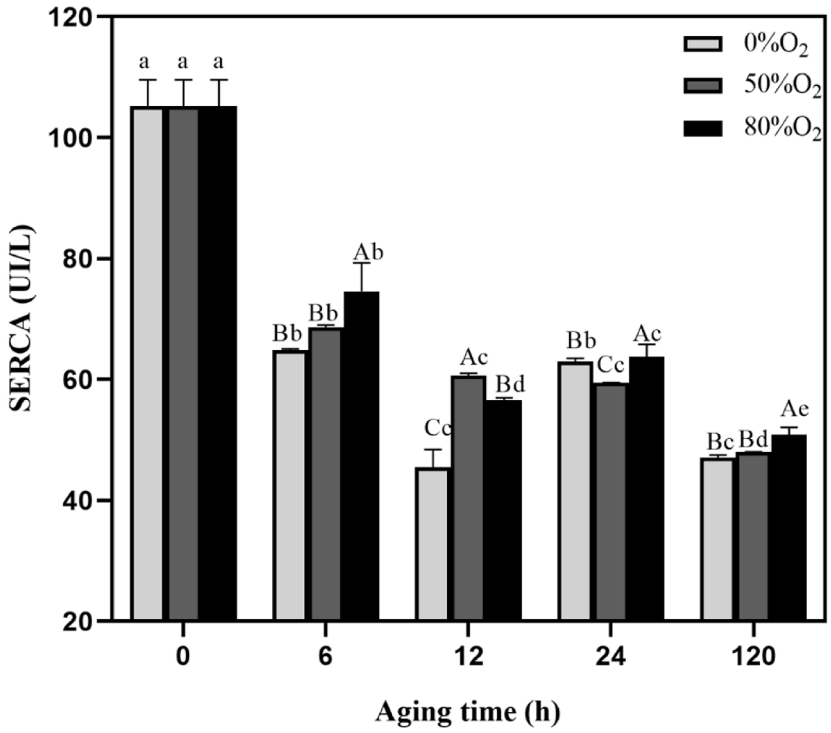

Fig. 1. (*continued*).

oxygen consumption of yak meat decreased with increasing oxygen concentration.

To determine the relationship between yak meat and oxygen consumption, we further investigated the oxygen penetration depth during postmortem aging in yak muscles. Furthermore, the oxygen penetration depth is another proof of oxygen consumption during post-mortem aging of yak meat, because, under a higher oxygen atmosphere, the meat will form a thicker and deeper OxyMb penetration layer. High

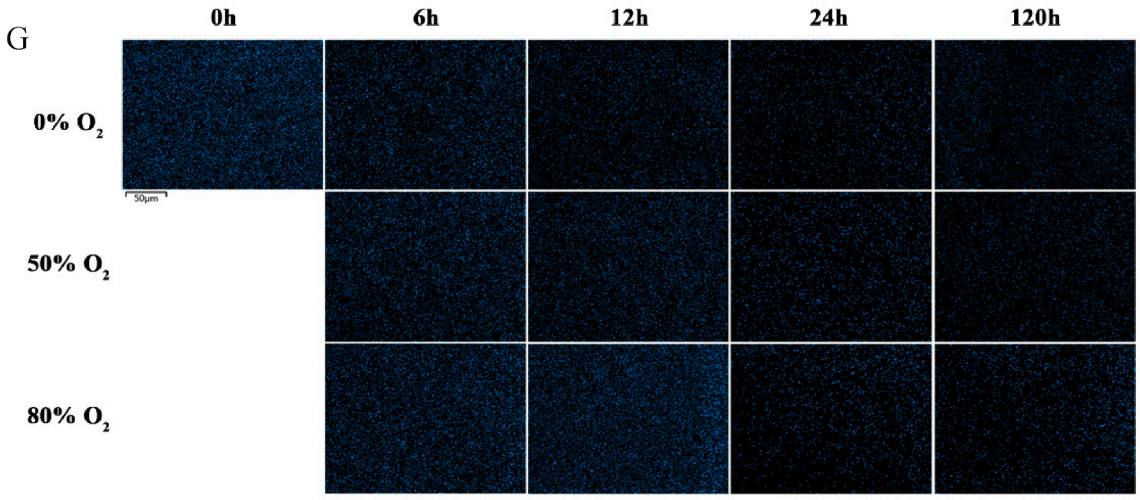

Fig. 1. (*continued*).

mitochondrial activity and swelling compete for oxygen, thereby limiting the penetration of oxygen to impair its deep penetration into the meat (Lu et al., 2020; Ramanathan et al., 2019). Thus, we assessed the oxygen concentration in yak muscles with aging time using oxygen penetration depth (Table 1). The data showed that oxygen penetration depth gradually increased with aging time ($P < 0.05$), indicating that oxygen gradually penetrates the yak muscle tissue during postmortem aging. Our study showed that an oxygen penetration depth of 80 % O_2-HiOx-MAP packaging and 50 % O_2-HiOx-MAP packaging enhanced ($P < 0.05$) as the postmortem aging was significantly higher than 0 % O_2-HiOx-MAP packaging. Among them, the 80 % O_2-HiOx-MAP packaging group was 0.31 nm higher than 50 % O_2-HiOx-MAP packaging group and 5.88 nm higher than 0 % O_2-HiOx-MAP packaging group at 120 h.

3.2. Determination of hypoxia-inducible factor (HIF-1α) and proline hydroxylases (PHD) from yak muscle during postmortem aging

Hypoxia-inducible factor (HIF-1α) is encoded by a potent inducer that is expressed under hypoxia conditions. HIF-1α is a transcription factor that regulates the expression of hypoxia-adaptive genes; it is a major protein that controls oxygen transport and utilization. Moreover, proline hydroxylases (PHD) precisely regulate HIF-1α and oxygen sensors via the intracellular hypoxia response pathway (Kataria et al., 2019). The HIF-1α expression of 80 % O_2-HiOx-MAP and 50 % O_2-HiOx-MAP group of yak meat in postmortem processing by western blotting is shown in Fig. 1A, B. The changes in the HIF-1α expression were significantly different ($P < 0.05$) under different oxygen concentrations of yak muscles before postmortem at 24 h. The HIF-1α expression of yak muscle were first increased from 0 h to 120 h, followed by a decrease with an increase in the postmortem aging in Fig. 1B ($P < 0.05$). However, the HIF-1α expression in different groups showed a significant difference and significantly decreased with increasing oxygen concentration ($P < 0.05$) as shown in Fig. 1. In addition, we investigated the activity of PHD to verify whether oxygen concentration was related to HIF-1α. Fig. 1C reflects the PHD activity during postmortem aging in yak muscles. The PHD activity in yak muscles significantly decreased with increasing postmortem aging; however, the 80 % O_2-HiOx-MAP packaging group of yak muscles significantly increased in other groups and reached the highest ($P < 0.05$). The result indicated showed the dependence of the PHD activity on oxygen concentration during postmortem aging and was positively correlated with our previous determination of oxygen consumption (Fig. 1C). Furthermore, the expression of HIF-1α increased significantly and the PHD activity decreased significantly with a decrease in oxygen consumption, showing a negative correlation between HIF-1α and PHD. This is consistent with the results of Kataria et al., (2019) who showed that the inhibition of prolyl hydroxylase activity (PHD) by dimethyl oxyglycine (DMOG) was induced by prolyl hydroxylase and proteasome pathway degradation of HIF-1α in hypoxic tumors. Vetrovoy and Rybnikova, (2019) demonstrated that the PHD can hydroxylate the proline residues in the ODD region of the amino terminus of HIF-1α. Moreover, it can rapidly bind to the pVHL protein and degrade it through the ubiquitin protease pathway. We have previously demonstrated that the expression of HIF-1α first increased and then decreased with an increase in the aging time. The HIF-1α of yak meat at different altitudes was proportional to the altitude (Xin et al., 2022). Wang et al. (2008) discovered that the HIF-1α induced the expression of genes that promote adaptation and survival of cells and whole organisms from normoxia (21 % O_2) to hypoxia (1 % O_2).

3.3. Changes in RyR expression and SERCA activity of high-concentration oxygen-packed yak meat during postmortem aging

Endoplasmic reticulum (ER) stress has been implicated in dysfunction-related apoptosis caused by Ca^{2+} homeostasis in the endoplasmic reticulum (Luciani et al., 2009). Ryanodine receptors (RyR) play a significant role in cellular hypoxia response, and calcium ions released from the sarcoplasmic/endoplasmic reticulum (SR/ER) exert a profound effect on PASMC hypoxia [Ca~(2 +)] and play a crucial role in elevating it (Song et al., 2017). Interestingly, HIF-1α-mediated destabilization of sarcoplasmic reticulum pressure triggers the activation of RyR, ultimately resulting in sarcoplasmic reticulum calcium release (Laver, 2018). Previous results demonstrated that packaging with different oxygen concentrations caused significant changes in the expression of HIF-1α during postmortem aging in yak meat (Fig. 1A and B; $P < 0.05$). Finally, we determined whether HIF-1α triggered the activation of ryanodine receptors protein RYR in postmortem yak muscle. The expression of RyR of 80 % O_2-HiOx-MAP and 50 % O_2-HiOx-MAP groups in yak meat was assessed. In Fig. 1D and E, the expression of RyR significantly increased before 24 h and subsequently decreased ($P < 0.05$). The maximum RyR expression was recorded at 24 h, whereas RyR expression in 80 % O_2-HiOx-MAP and 50 % O_2-HiOx-MAP treatment groups was significantly different when compared with the control ($P < 0.05$). In addition, the expression of RyR significantly decreased with increasing oxygen concentration when compared with the 80 % O_2-HiOx-MAP and 50 % O_2-HiOx-MAP treatment groups ($P < 0.05$). These results are similar to those reported by Liao et al. (2011), showing that the RyR activity gradually increased with increased expression of hypoxia HIF-1α in pulmonary artery myocytes. In addition, Lu et al. (2017) reported that the blocking of the RYR1 activity and calcium-dependent signaling could be achieved by inhibiting HIFs.

Table 2
Effects of oxygen concentrations and aging time on the ER Ca^{2+} concentration and MC Ca^{2+} concentration of yak during postmortem aging.

Parameters	Packaging	Aging time (h)				
		0	6	12	24	120
ER Ca^{2+} concentration (μmol/L)	0 $\%O_2$	8.11 ± 0.05^{e}	18.39 ± 0.01^{Cd}	31.82 ± 0.13^{Cc}	49.64 ± 0.05^{Cb}	93.79 ± 0.13^{Ca}
	50 $\%O_2$ + 50 $\%CO_2$	8.11 ± 0.05^{e}	21.72 ± 0.02^{Bd}	33.01 ± 0.14^{Bc}	51.10 ± 0.05^{Bb}	106.73 ± 0.24^{Ba}
	80 $\%O_2$ + 20 $\%CO_2$	8.11 ± 0.05^{e}	25.79 ± 0.03^{Ad}	38.78 ± 0.20^{Ac}	57.71 ± 0.16^{Ab}	122.76 ± 0.13^{Aa}
MC Ca^{2+}concentration (μmol/L)	0 $\%O_2$	1.36 ± 0.02^{b}	1.39 ± 0.01^{Cab}	1.41 ± 0.01^{Ca}	1.42 ± 0.01^{Ca}	1.27 ± 0.01^{Bc}
	50 $\%O_2$ + 50 $\%CO_2$	1.36 ± 0.02^{d}	1.44 ± 0.01^{Bc}	1.49 ± 0.01^{Bb}	1.61 ± 0.01^{Ba}	1.28 ± 0.02^{Be}
	80 $\%O_2$ + 20 $\%CO_2$	1.36 ± 0.02^{d}	1.52 ± 0.01^{Ac}	1.64 ± 0.01^{Ab}	1.79 ± 0.01^{Aa}	1.34 ± 0.01^{Ad}

Sarcoplasmic reticulum calcium-ATPase (SERCA) triggered the release of calcium channels to function downstream of the sarcoplasmic reticulum. It is an intracellular membrane-associated protease involved in intracellular calcium signaling and homeostasis (Tadini-Buoninsegni et al., 2018). The changes in the SERCA activity in different oxygen concentration packaging during aging are shown in Fig. 1F. The activity of SERCA significantly decreased with the increasing aging time ($P < 0.05$); however, it became insignificant ($P > 0.05$) during aging in the 80 % O_2-HiOx-MAP and 50 % O_2-HiOx-MAP groups. However, the reduced rate of the SERCA activity in the 0 % O_2-HiOx-MAP group was significantly higher than in the 80 % O_2-HiOx-MAP and 50 % O_2-HiOx-MAP groups at 12 h ($P < 0.05$). This result could be ascribed to the changes in the expression of HIF-1 because sarcoplasmic reticulum Ca^{2+} homeostasis is thought to be related to HIF-1α, resulting in the regulation of SERCA2 expression (Williams et al., 2019). Furthermore, according to Ronkainen, Skoumal, & Tavi (2011), the effect of hypoxia on the expression of SERCA is mediated by HIF-1, and the SERCA2a promoter contains two putative HIF-1 binding HRE sites. These results further support the function of SERCA and RyR expression in the relationship between postmortem maturation and HIF-1α. In addition, consistent with previous studies mentioned above, the results of this study report that in postmortem bovine muscles, the oxygen concentration was negatively correlated with RyR expression and positively correlated with SERCA activity. Moreover, HIF-1α constitutes a major component of hypoxia response, which is consistent with previous studies on the function of HIF-1α in mediating the hypoxia response of the ER (Lu et al., 2017).

3.4. *Changes in endoplasmic reticulum Ca^{2+} levels and distribution of yak meat during postmortem aging*

Impaired SERCA function can cause increased intracellular calcium concentration and altered calcium homeostasis, thereby triggering endoplasmic reticulum (ER) stress (Oyadomari and Mori, 2004). Changes in the calcium ion concentration can be used to evaluate the degree of stress in the ER. Increased endoplasmic reticulum calcium concentration reflects an increased ER opening (Cardozo et al., 2005). Therefore, we observed the calcium distribution and concentration in

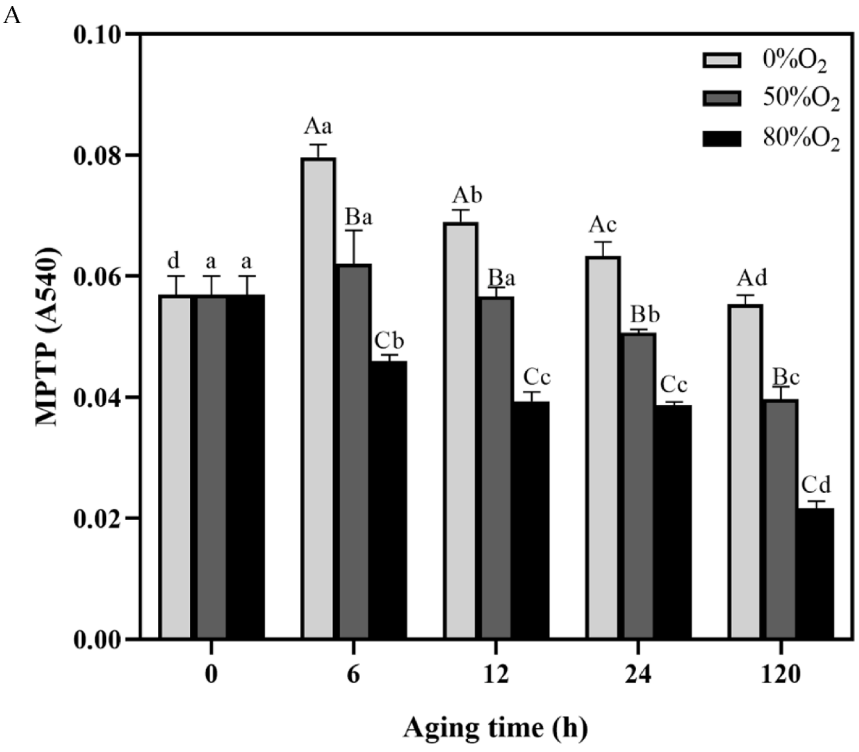

Fig. 2. (A) The absorbance values of membrane permeability transition pore (MPTP) opening in 0 % O_2-HiOx-MAP, 50 % O_2-HiOx-MAP and 80 % O_2-HiOx-MAP groups. The absorbance values in yak meat in the three groups stored at 4 °C for 0, 6, 12, 24, and 120 h as shown. (B) Representative ΔΨm in 0 % O_2-HiOx-MAP, 50 % O_2-HiOx-MAP and 80 % O_2-HiOx-MAP groups. Changes in mitochondrial membrane potential as shown by the red/green fluorescence intensity ratio with JC-1 aye. (C) The distribution of mitochondrial calcium in 0 % O_2-HiOx-MAP, 50 % O_2-HiOx-MAP and 80 % O_2-HiOx-MAP groups and yellow fluorescence expressed Ca^{2+}. Note: The capital letters represent the difference of all treatment groups and the lowercase letters represent stands the difference of the postmortem aging ($P < 0.05$). Error bars indicate the standard errors of the mean. (For interpretation of the references to color in this figure legend, the reader is referred to the web version of this article.)

B

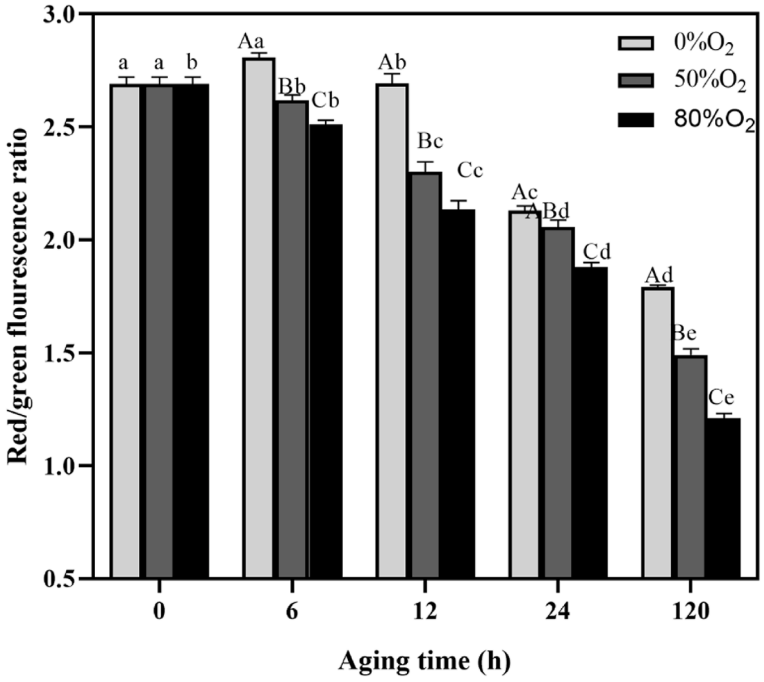

C

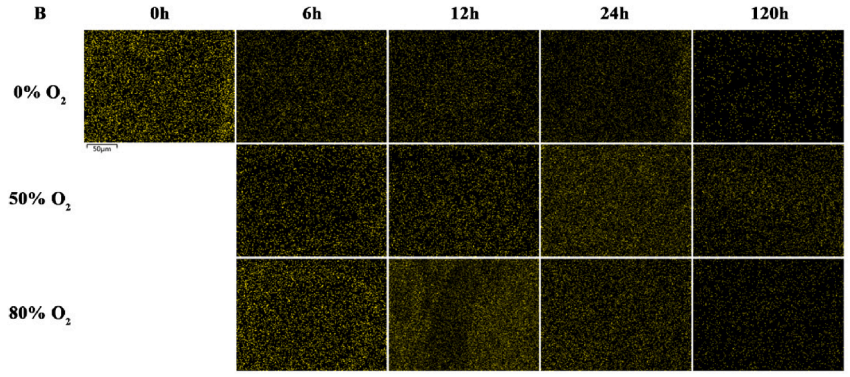

Fig. 2. (*continued*).

the endoplasmic reticulum. In our study, the Ca^{2+} concentration of ER significantly increased ($P < 0.05$) from 0 h to 120 h as shown in Table 2, demonstrating that the calcium release from the ER is an irreversible physiological state during the postmortem aging process. The distribution of sarcoplasmic reticulum calcium was labeled with green fluorescence in postmortem bovine muscles (Fig. 1G). The distribution of ER calcium was reduced at 0 to 120 h aging time. In addition, the endoplasmic reticulum Ca^{2+} concentration in the control group were lower than 80 % O_2-HiOx-MAP and 50 % O_2-HiOx-MAP treatment group ($P < 0.05$) from 6 h to 120 h. Consistently, the endoplasmic reticulum Ca^{2+} concentration in 50 % O_2-HiOx-MAP was significantly lower than that of 80 % O_2-HiOx-MAP from 6 h to 120 h, and the highest endoplasmic reticulum Ca^{2+} levels in 80 % O_2-HiOx-MAP group were 13.06 % higher than those of 50 % O_2-HiOx-MAP packaging, and 23.6 % higher than those of the control group ($P < 0.05$; Table 2). Hypoxic cells have important functions in maintaining a negative membrane potential and providing an electrical driving force that controls the calcium influx in a HIF-1α-dependent manner under hypoxic conditions (Shin et al., 2014). HIF-1α promotes ER calcium release by regulating the expression of glutathione S-transferase omega-1 (GSTO1), which interacts with ranidin receptor 1 (RYR1) (Lu et al., 2017). HIF-1-mediated CA1 and CA3 neuron-specific SERCA can modulate neuronal intracellular calcium storage dysfunction (Kopach et al., 2016). In addition, we found that the expression of ryanodine receptors (RyR) in the packaging group with high oxygen concentration was lower than in other groups, whereas the SERCA activity was higher than that of other groups. This result also demonstrated that the ability of the endoplasmic reticulum to release calcium ions into the cytoplasm increased as the HIF-1α increased, whereas the ability to return to the endoplasmic reticulum to store calcium ions decreased.

3.5. Changes in mitochondrial apoptosis pathways of high oxygen-modified packaging (HiOx-MAP) yak muscle during postmortem aging

The mitochondrial apoptosis pathway has been implicated in the tenderization of meat (Wang et al., 2018). We studied whether HIF-1α

A

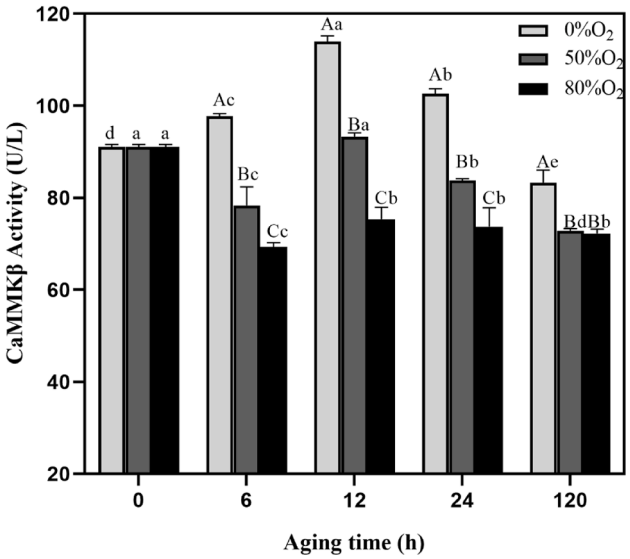

Fig. 3. (A) The activity of calmodulin protein (CaMKKβ) in 0 % O_2-HiOx-MAP, 50 % O_2-HiOx-MAP and 80 % O_2-HiOx-MAP groups. The activity of CaMKKβ in yak meat in the three groups stored at 4 °C for 0, 6, 12, 24, and 120 h as shown. (B) The activity of AMP-activated protein kinase (AMPK) in 0 % O_2-HiOx-MAP, 50 % O_2-HiOx-MAP and 80 % O_2-HiOx-MAP groups. The activity of AMPK in yak meat in the three groups stored at 4 °C for 0, 6, 12, 24, and 120 h as shown. (C) The qualitative analysis by immunofluorescence of CaMKKβ and AMPK in 0 % O_2-HiOx-MAP, 50 % O_2-HiOx-MAP and 80 % O_2-HiOx-MAP groups. The distribution of CaMKKβ and AMPK in yak meat in the three groups stored at 4 °C for 0, 6, 12, 24, 120 h as shown, red expressed the position of CaMKKβ and green expressed the position of AMPK. (D) The activity of caspase-9 in 0 % O_2-HiOx-MAP, 50 % O_2-HiOx-MAP and 80 % O_2-HiOx-MAP groups. The activity of caspase-9 in yak meat in the three groups stored at 4 °C for 0, 6, 12, 24, and 120 h as shown. (E) The activity of caspase-3 in 0 % O_2-HiOx-MAP, 50 % O_2-HiOx-MAP and 80 % O_2-HiOx-MAP groups. The activity of caspase-3 in yak meat in the three groups stored at 4 °C for 0, 6, 12, 24, and 120 h as shown. Note: The capital letters represent the difference of all treatment groups and the lowercase letters represent stands the difference of the postmortem aging ($P < 0.05$). Error bars indicate the standard errors of the mean. (For interpretation of the references to color in this figure legend, the reader is referred to the web version of this article.)

could regulate yak meat tenderness through the mitochondrial apoptosis pathway. We first investigated the effects of 80 % O_2-HiOx-MAP packaging, 50 % O_2-HiOx-MAP packaging group, and control group on the state of the mitochondrial structure during postmortem aging of yak meat as shown in Fig. 2. The MPTP opening and mitochondrial membrane potential (ΔΨm) of all groups decreased significantly with an increase in the aging time ($P < 0.05$; Fig. 2A and B). This result is consistent with that obtained by Wang et al. (2018), indicating that the damage to the mitochondrial structure in the postmortem maturation process of yak muscle is irreversible. The mitochondrial apoptosis reflects a decreased trend in the postmortem process, showing that mitochondrial swelling was enhanced with an increase in the aging time. Furthermore, the ΔΨm in the 0 % O_2-HiOx-MAP group at 6 h to 120 h was significantly higher than the 80 % O_2-HiOx-MAP and 50 % O_2-HiOx-MAP group ($P < 0.05$), and we found that the expression of HIF-1α and the calcium concentration in the endoplasmic reticulum (ER) decreased with an increase in the oxygen concentration in this study ($P < 0.05$), which is attributed to the increased intracellular calcium, which is responsible for the decrease in ΔΨm (Festjens et al., 2004). The absorbance significantly decreased ($P < 0.05$) with package oxygen concentration, which represented increased MPTP openness. The mitochondrial permeability transition pore (MPTP) opening causes the loss of ΔΨ (Mnatsakanyan et al., 2017), and the entry of cellular calcium across the inner mitochondrial membrane increases the concentration of calcium ions in the mitochondria during postmortem aging (Saotome et al., 2005). Therefore, we determined the calcium ion concentration and distribution in the mitochondria as shown in Fig. 2C and Table 2. In addition, mitochondrial Ca^{2+} concentration of all groups enhanced in 0–24 h and then reached to the maximum values at 24 h of 1.42 (0 % O_2-HiOx-MAP), 1.61 (50 % O_2-HiOx-MAP), and 1.79 μmol/L (80 % O_2-HiOx-MAP), respectively, whereas it declined at 120 h ($P < 0.05$; Table 2). As shown in Fig. 2C, the distribution of calcium in the mitochondria in postmortem yak muscle was marked by yellow fluorescence distribution of calcium in the mitochondria showed a downward trend from 0 to 120 h. In addition, Ca^{2+} levels in the control group were lower than in other high-oxygen packing groups ($P < 0.05$; Table 2), demonstrating again that HIF-1α is inversely correlated with mitochondrial calcium concentration.

3.6. Changes in CaMKKβ and AMPK activity of high oxygen-modified packaging (HiOx-MAP) yak meat during postmortem aging

AMPK (AMP-activated protein kinase, AMPK) is an AMP-activated protein kinase, a heterotrimer composed of a catalytic subunit (α) and two regulatory subunits (β and γ). Certain scholars have reported that AMPK induces mitochondrial dysfunction and apoptosis (Monteverde et al., 2015, Faubert et al., 2015). In addition, calcium/calmodulin-dependent protein kinase is an important calcium-modulating protein and is the only upstream kinase of AMPK regulated by Ca^{2+} release (Morales-Alamo et al., 2012). Calmodulin protein (CaMKKβ) is immediately activated when free Ca^{2+} levels in the cytoplasm increase (Hawley et al., 1995). We found that sarcoplasmic calcium ions increased with increasing HIF-1α expression during postmortem maturation; therefore, we investigated the activities of CaMKKβ and AMPK, both of which are abundant in the cytoplasm. The activity of CaMKKβ and AMPK in all groups significantly increased in 0–12 h and subsequently decreased at 24–120 h (Fig. 3A and B; $P < 0.05$). The CaMKKβ activity of the control group was 83.32 U/L and decreased to 72.27 μmol/L in the 80 % O_2-HiOx-MAP packaging group at 120 h postmortem (Fig. 3A). The alternative pathway of AMPK activation triggered following an increase in the cytoplasmic Ca^{2+} concentration activated CaMKKβ, which can phosphorylate the Thr172 site on the AMPK α

B

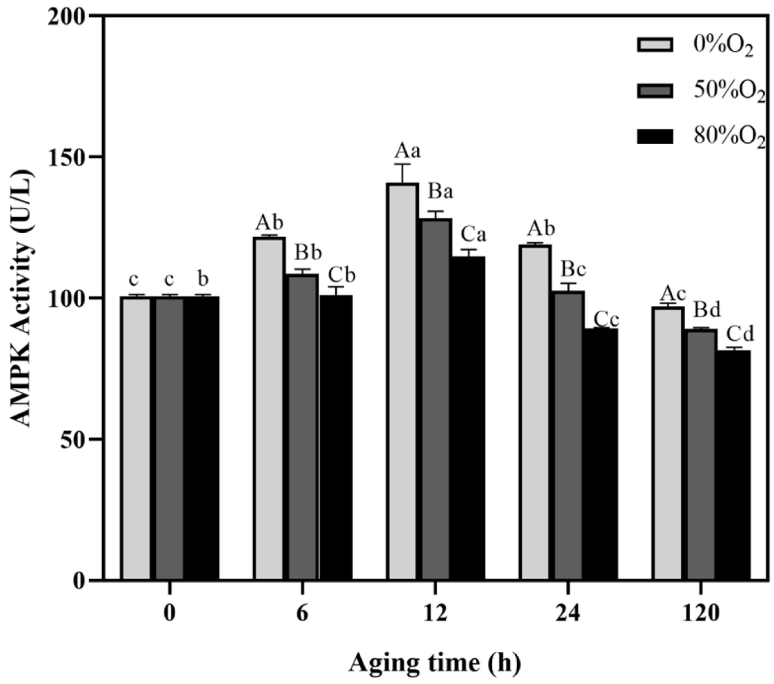

C

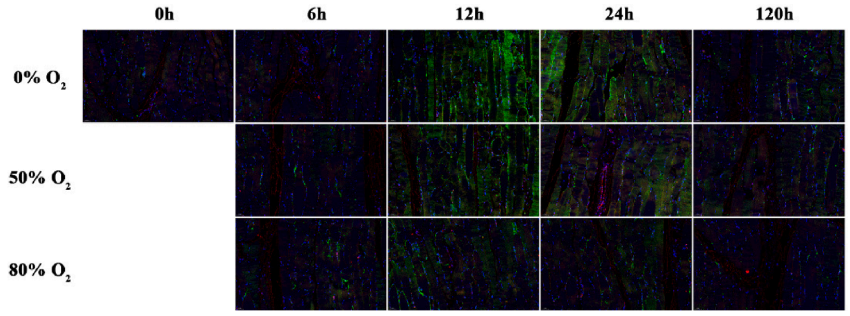

Fig. 3. (*continued*).

subunit, thereby activating AMPK (Angela et al., 2005). In addition, the AMPK activity of the control group at postmortem 0 h was 100.37 U/L, which decreased to 97.01 U/L at 120 h, and the AMPK activity of the 50 % O_2-HiOx-MAP packaging group decreased to 89.02 U/L at postmortem 120 h, and the AMPK activity of the 80 % O_2-HiOx-MAP packaging group decreased to 81.55 U/L at postmortem 120 h (Fig. 3B). To further analyze the changes in AMPK and CaMKKβ activities, we performed qualitative analysis by immunofluorescence and found that the changing trend and activity of AMPK and CaMKKβ during post-mortem maturation were consistent (Fig. 3C). This is consistent with Gao et al. (2019), which found that high-altitude yak meat exerted a strong energy metabolic activity after slaughter and AMPK activation, entering rigidity earlier and completing maturation. Certain scholars believe that intermittent hypoxia can cause transient AMPK activation, which inhibits apoptosis to protect cells (Faubert et al., 2015; Kilic et al., 2007). This is because AMPK could continue to provide energy for cells under hypoxia by promoting the transfer of GLUT1 to the cell membrane, and phosphorylating transcription factors to induce the uptake and transport of glucose (Winder, & Hardie, 1999). Our results confirmed that the rate of glycolysis was proportional to the expression of HIF-1α and GLUT-1 expression during postmortem aging of yak meat (Xin et al., 2022).

3.7. Changes in caspase-enzyme activities and apoptotic nucleus counts in high oxygen-modified packaging (HiOx-MAP) of yak meat in postmortem process

The MPTP opening and ΔΨm increased with increasing oxygen concentration during the postmortem aging period ($P < 0.05$; Fig. 2A and B). Moreover, the AMPK activity was inversely proportional to oxygen concentration in Fig. 3B ($P < 0.05$). All results showed that HIF-1α is not only involved in the energy metabolism pathway in the postmortem maturation of yak muscle but may also regulate the mitochondrial apoptosis pathway and affect meat tenderness. The mitochondrial pathway releases cytochrome *c* and combines to apaf-1, activates pro-aspartic protease-3, and initiates apoptosis during the postmortem maturation of yak meat (Wang et al., 2018). We proved this hypothesis by measuring apoptotic nucleus counts and apoptotic enzyme activities. The changes in the caspase-9 activity of the three groups increased significantly during the whole postmortem aging period (Fig. 3D). The caspase-9 activity of the 80 % O_2-HiOx-MAP

D

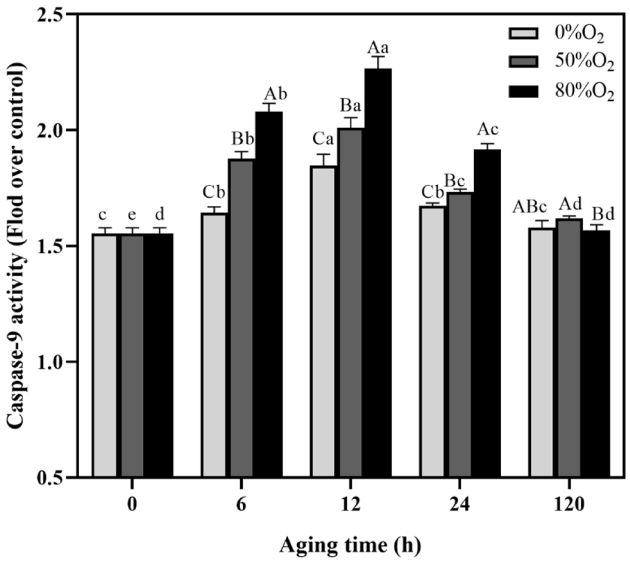

E

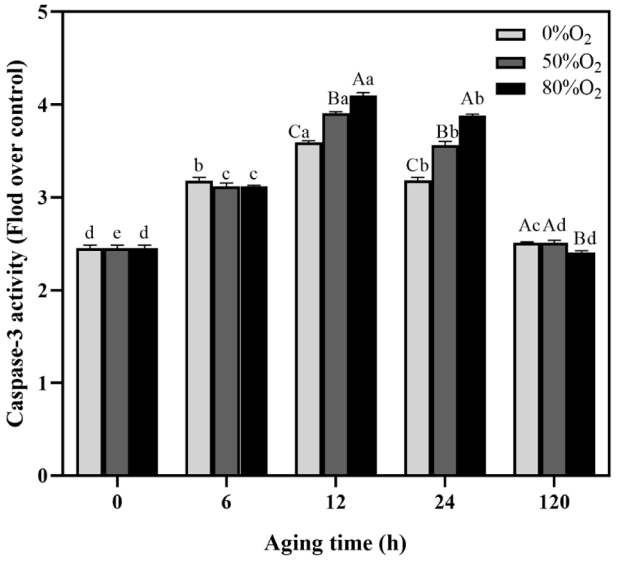

Fig. 3. (*continued*).

packaging group significantly increased in the 50 % O_2-HiOx-MAP packaging and control groups ($P < 0.05$; Fig. 3D) from 6 h to 24 h. The caspase-3 in the 0 % O_2-HiOx-MAP group was significantly higher than at 12 to 24 h in the 80 % O_2-HiOx-MAP and 50 % O_2-HiOx-MAP packaging group; however, 80 % O_2-HiOx-MAP packaging group significantly decreased at 120 h ($P < 0.05$). The count of apoptotic nuclei significantly increased by aging in all groups (Fig. 4A and B), and the three groups showed a significant difference at various aging times ($P < 0.05$). The apoptotic nucleus counts of all groups, respectively, were 11 %, 25 %, 46.3 % at 120 h (Fig. 4A and B). These results indicate that the lower expression of HIF-1α (high oxygen concentration) significantly promoted apoptosis. Sasabe et al. (2005) suggested that the overexpression of HIF-1α inhibited the accumulation of cytochrome *c*, resulting in the inactivation of caspase-9. The Bcl2 family proteins regulate cytochrome *c* release; however, the expression of anti-apoptotic Bcl2 and Bclxl increased and the expression of pro-apoptotic bax and Bak decreased in HIF-1α-overexpressing oral squamous cell hypoxic cell lines (Festjens et al., 2004). These findings proved that HIF-1α inhibits apoptosis.

3.8. Changes in myofibril fragmentation index (MFI) of high oxygen-modified packaging (HiOx-MAP) yak muscle in postmortem aging process

The HIF-1α expression is highly essential for the mitochondrial apoptosis pathway during postmortem aging. Therefore, we further investigated whether postmortem yak muscle tenderness was altered in the presence of high oxygen concentration suppressing the expression of HIF-1α. The relationship between beef tenderness and myofibril fragmentation index (MFI) was quantified, which showed a high correlation and MFI accounts for approximately 50 % of changes in tenderness (Rajagopal, & Oommen, 2015). This experiment proved that the MFI in 50 % O_2-HiOx-MAP and 80 % O_2-HiOx-MAP packed with hyperoxia significantly increased during postmortem aging. The MFI was 79.23 in the control group, 94.29 in the 50 % O_2-HiOx-MAP packaging group, and reached 108.16 in the 80 % O_2-HiOx-MAP packaging group at the end of postmortem aging (Fig. 4C). This implied that with an increase in

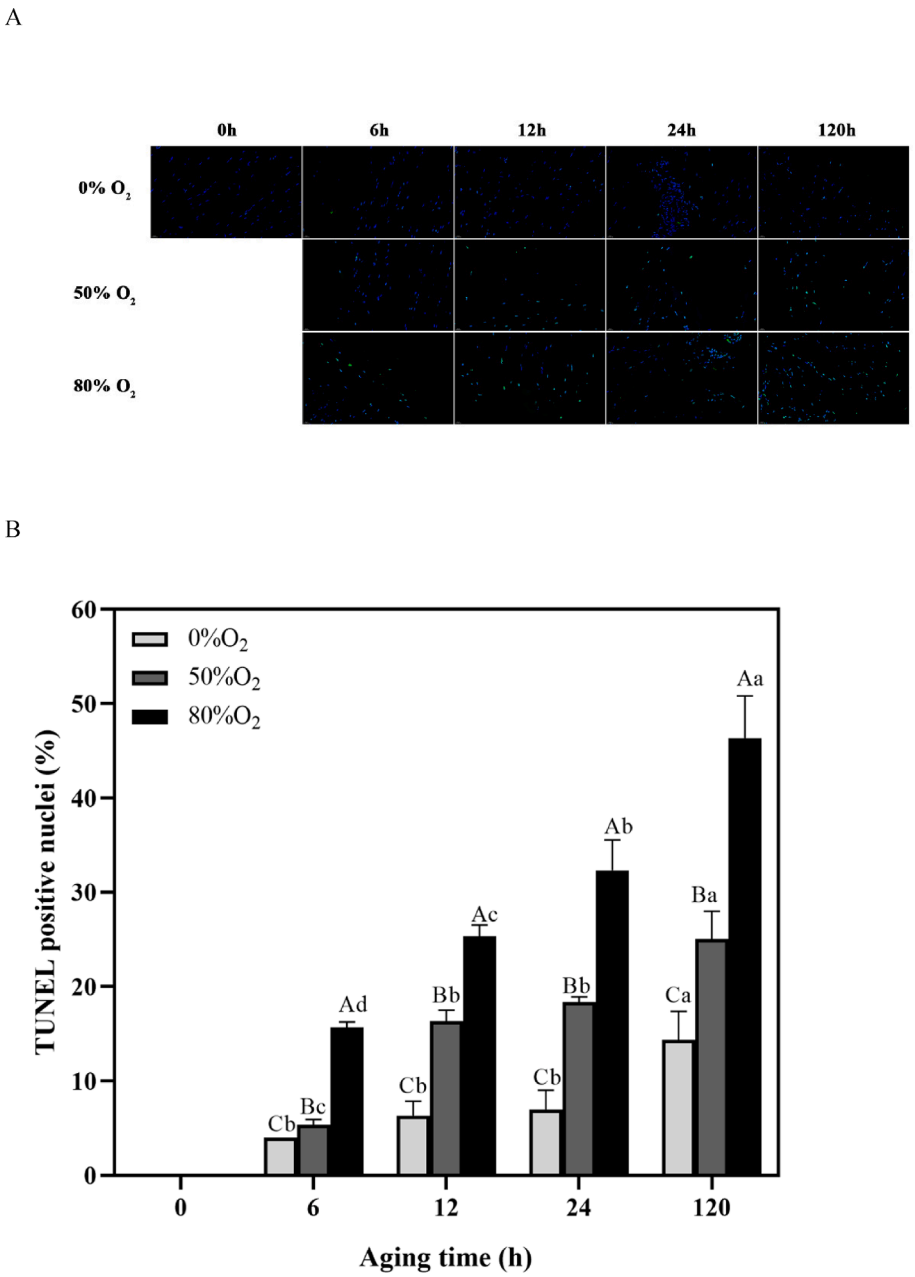

Fig. 4. (A/B) The apoptotic nucleus counts in in 0 % O_2-HiOx-MAP, 50 % O_2-HiOx-MAP and 80 % O_2-HiOx-MAP groups. Blue is nucleus, green is apoptotic nucleus and then the apoptosis rate was analyzed using the positive nuclei number in per whole sample section. (C) Representative the myofibril fragmentation index (MFI) in 0 % O_2-HiOx-MAP, 50 % O_2-HiOx-MAP and 80 % O_2-HiOx-MAP groups stored at 4 °C for 0, 6, 12, 24, and 120 h as shown. Note: The capital letters represent the difference of all treatment groups and the lowercase letters represent stands the difference of the postmortem aging ($P < 0.05$). Error bars indicate the standard errors of the mean. (For interpretation of the references to color in this figure legend, the reader is referred to the web version of this article.)

the oxygen concentration, the tenderness of yak meat increased during postmortem maturation. Thus, to improve the yak meat tenderness, the expression of HIF-1α can be decreased by increasing the oxygen concentration during postmortem process.

4. Conclusion

We observed an increase in the tenderness of yak meat following high oxygen-modified packaging during postmortem aging of yak meat as shown in Fig. 5. Decreased expression of hypoxia-inducible factor (HIF-1α) is an important factor in inducing apoptosis. In addition, high oxygen-modified packaging reduced the expression of HIF-1α and increased the activity of proline hydroxylase (PHD) during early postmortem aging, the endoplasmic reticulum (ER) calcium concentration increased with increasing oxygen concentration. The high oxygen-modified packaging inhibited the expression of HIF-1α to upregulate the inner mitochondrial Ca^{2+} concentration, which in turn activates caspase-9 and caspase-3, leading to apoptosis. In addition, lower expression of HIF-1α inhibits the release of calcium ions from the endoplasmic reticulum into the sarcoplasm and downregulates the activity of calmodulin protein (CaMKKβ) and AMP-activated protein kinase (AMPK) to promote apoptosis. This result indicated that high-concentration oxygen packaging downregulates the expression of HIF-1α in yak meat during postmortem maturation, induces apoptosis, and

C

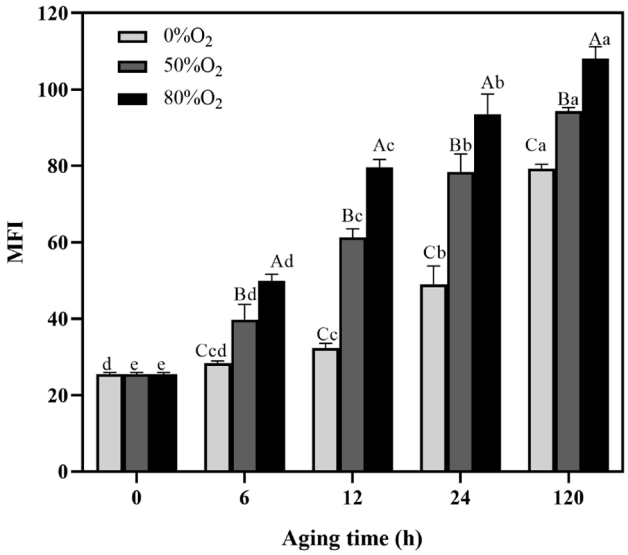

Fig. 4. (*continued*).

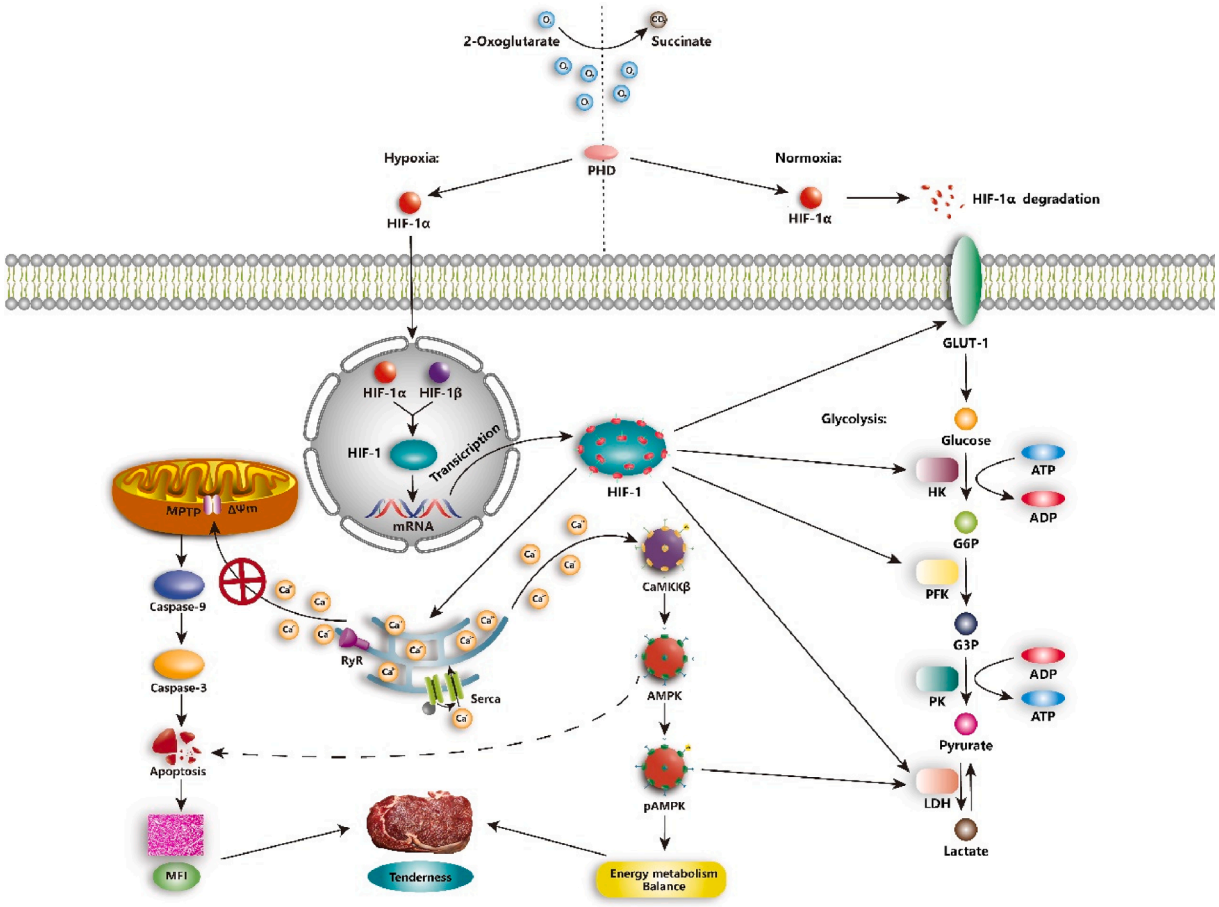

Fig. 5. Working model of High oxygen modified packaging (HiOx-MAP) mediates HIF-1α regulation of tenderness changes during postmortem aging of yak meat.

improves the tenderness of yak meat. Moreover, the postmortem relationship between HIF-1α and mitochondrial stability, apoptosis, and tenderness remains unclear and requires further investigation. Altogether, we believe our study provides new insights into the tenderization of muscle cell apoptosis during postmortem aging. Modified atmosphere packaging is expected to improve meat tenderness during postmortem aging, which is highly significant in enhancing the meat market value.

Ethical approval

Ethics approval was not required for this research.

CRediT authorship contribution statement

Ke-qi Xin: Investigation, Methodology, Software, Validation. **Kai Tian:** Resources, Formal analysis. **Qun-li Yu:** Conceptualization, Supervision, Validation, Project administration. **Ling Han:** Conceptualization, Supervision, Validation, Project administration.

Declaration of Competing Interest

The authors declare that they have no known competing financial interests or personal relationships that could have appeared to influence the work reported in this paper.

Data availability

The authors are unable or have chosen not to specify which data has been used.

Acknowledgments

The work was supported by the National Natural Science Foundation of China (No. 32060553), National Key Research and Development (No. 2021YFD1600204-2), and the industrialization of the Cascade Processing of Ecological Beef and Mutton (No. 2020C-18).

References

AMSA. (2012). *AMSA meat color measurement guidelines* (vol. 61820). Champaign, Illinois USA: American Meat Science Association.

Angela, W., Kristina, D., Richard, H., Seung-Pyo, H., Milica, M., Stephen, R. J., Marian, C., & David, C. (2005). Ca2+/calmodulin-dependent protein kinase kinase-β acts upstream of AMP-activated protein kinase in mammalian cells. *Cell Metabolism, 2*, 21–33.

Cardozo, A. K., Ortis, F., Storling, J., Feng, Y. M., Rasschaert, J., Tonnesen, M., … Eizirik, D. L. (2005). Cytokines downregulate the sarcoendoplasmic reticulum pump Ca2+ ATPase 2b and deplete endoplasmic reticulum Ca2+, leading to induction of endoplasmic reticulum stress in pancreatic β-cells. *Diabetes, 54*(2), 452–461.

Chen, L., Feng, X.-C., Zhang, Y.-Y., Liu, X.-B., Zhang, W.-G., Li, C.-B., … Zhou, G.-H. (2015). Effects of ultrasonic processing on caspase-3, calpain expression and myofibrillar structure of chicken during post-mortem ageing. *Food Chemistry, 177*, 280–287.

Chen, X., Cho, D. B., & Yang, P. C. (2010). Double staining immunohistochemistry. *North American Journal of Medical Sciences, 2*(5), 241.

Dong, Z., Venkatachalam, M. A., Wang, J., Patel, Y., Saikumar, P., Semenza, G. L., … Nishiyama, J. (2001). Up-regulation of apoptosis inhibitory protein IAP-2 by hypoxia: HIF-1-independent mechanisms. *Journal of Biological Chemistry, 276*(22), 18702–18709.

Festjens, N., van Gurp, M., van Loo, G., Saelens, X., & Vandenabeele, P. (2004). Bcl-2 family members as sentinels of cellular integrity and role of mitochondrial intermembrane space proteins in apoptotic cell death. *Acta haematologica, 111*(1–2), 7–27.

Faubert, B., Vincent, E. E., Poffenberger, M. C., & Jones, R. G. (2015). The AMP-activated protein kinase (AMPK) and cancer: Many faces of a metabolic regulator. *Cancer Letters, 356*, 165–170.

Fulda, S., & Debatin, K. M. (2007). HIF-1-regulated glucose metabolism: A key to apoptosis resistance? *Cell Cycle, 6*(7), 790–792.

Greijer, A. E., & Van der Wall, E. (2004). The role of hypoxia inducible factor 1 (HIF-1) in hypoxia induced apoptosis. *Journal of Clinical Pathology, 57*(10), 1009–1014.

Gao, Y., Yang, Y., Han, L., Yu, Q., Song, R., Han, M., … He, L. (2019). Study on the effect of CaMKKβ-mediated AMPK activation on the glycolysis and the quality of different altitude postmortem bovines longissimus muscle. *Journal of Food Biochemistry, 43*(11), e13023.

Hawley, S. A., Selbert, M. A., Goldstein, E. G., Edelman, A. M., Carling, D., & Hardie, D. G. (1995). 5′-AMP activates the AMP-activated protein kinase cascade, and Ca2+/calmodulin activates the calmodulin-dependent protein kinase I cascade, via three independent mechanisms. *Journal of Biological Chemistry, 270*(45), 27186–27191.

Hopkins, D. L. The eating quality of meat: II-Tenderness. Lawrie's Meat Science eight edition. Woodhead Publishing Series in Food Science, 2017, pp. 357-381.

Kopach, O., Maistrenko, A., Lushnikova, I., Belan, P., Skibo, G., & Voitenko, N. (2016). HIF-1α-mediated upregulation of SERCA2b: The endogenous mechanism for alleviating the ischemia-induced intracellular Ca2+ store dysfunction in CA1 and CA3 hippocampal neurons. *Cell Calcium, 59*(5), 251–261.

Kilic, M., Kasperczyk, H., Fulda, S., & Debatin, K. M. (2007). Role of hypoxia inducible factor-1 alpha in modulation of apoptosis resistance. *Oncogene, 26*, 2027–2038.

Khan, A. A., Soloski, M. J., Sharp, A. H., Schilling, G., Sabatini, D. M., Li, S. H., … Snyder, S. H. (1996). Lymphocyte apoptosis: Mediation by increased type 3 inositol 1, 4, 5-trisphosphate receptor. *Science, 273*(5274), 503–507.

Kaluz, S., Zhang, Q., Kuranaga, Y., Yang, H., Osuka, S., Bhattacharya, D., … Van Meir, E. G. (2021). Targeting HIF-activated collagen prolyl 4-hydroxylase expression disrupts collagen deposition and blocks primary and metastatic uveal melanoma growth. *Oncogene, 40*(33), 5182–5191.

Kataria, N., Martinez, C. A., Kerr, B., Zaiter, S. S., Morgan, M., McAlpine, S. R., & Cook, K. M. (2019). C-terminal HSP90 inhibitors block the HIF-1 hypoxic response by degrading HIF-1α through the oxygen-dependent degradation pathway. *Cellular Physiology and Biochemistry, 53*(3), 480–495.

Liao, B., Zheng, Y. M., Yadav, V. R., Korde, A. S., & Wang, Y. X. (2011). Hypoxia induces intracellular Ca2+ release by causing reactive oxygen species-mediated dissociation of FK506-binding protein 12.6 from ryanodine receptor 2 in pulmonary artery myocytes. *Antioxidants & Redox Signaling, 14*(1), 37–47.

Luciani, D. S., Gwiazda, K. S., Yang, T. L. B., Kalynyak, T. B., Bychkivska, Y., Frey, M. H., … Johnson, J. D. (2009). Roles of IP3R and RyR Ca2+ channels in endoplasmic reticulum stress and β-cell death. *Diabetes, 58*(2), 422–432.

Laver, D. R. (2018). Regulation of the RyR channel gating by Ca2+ and Mg2+. *Biophysical Reviews, 10*(4), 1087–1095.

Lu, H., Chen, I., Shimoda, L. A., Park, Y., Zhang, C., Tran, L., … Semenza, G. L. (2017). Chemotherapy-induced Ca2+ release stimulates breast cancer stem cell enrichment. *Cell Reports, 18*(8), 1946–1957.

Lu, X., Cornforth, D. P., Carpenter, C. E., Zhu, L., & Luo, X. (2020). Effect of oxygen concentration in modified atmosphere packaging on color changes of the M. longissimus thoraces et lumborum from dark cutting beef carcasses. *Meat Science, 161*, Article 107999.

Li, J. X., Tong, C. W. C., Xu, D. Q., & Chan, K. M. (1999). Changes in membrane fluidity and lipid peroxidation of skeletal muscle mitochondria after exhausting exercise in rats. *European Journal of Applied Physiology and Occupational Physiology, 80*(2), 113–117.

López-Arce, P., Gómez-Villalba, L. S., Martínez-Ramírez, S., De Buergo, M.Á., & Fort, R. (2011). Influence of relative humidity on the carbonation of calcium hydroxide nanoparticles and the formation of calcium carbonate polymorphs. *Powder Technology, 205*(1–3), 263–269.

Mnatsakanyan, N., Beutner, G., Porter, G. A., Alavian, K. N., & Jonas, E. A. (2017). Physiological roles of the mitochondrial permeability transition pore. *Journal of Bioenergetics and Biomembranes, 49*(1), 13–25.

Monteverde, T., Muthalagu, N., Port, J., & Murphy, D. J. (2015). Evidence of cancer-promoting roles for AMPK and related kinases. *The FEBS Journal, 282*(24), 4658–4671.

Morales-Alamo, D., Ponce-González, J. G., Guadalupe-Grau, A., Rodríguez-García, L., Santana, A., Cusso, M. R., … Calbet, J. A. (2012). Increased oxidative stress and anaerobic energy release, but blunted Thr172-AMPKα phosphorylation, in response to sprint exercise in severe acute hypoxia in humans. *Journal of Applied Physiology, 113*(6), 917–928.

MacLennan, D. H. (1970). Purification and properties of an adenosine triphosphatase from sarcoplasmic reticulum. *Journal of Biological Chemistry, 245*(17), 4508–4518.

Oyadomari, S., & Mori, M. (2004). Roles of CHOP/GADD153 in endoplasmic reticulum stress. *Cell Death & Differentiation, 11*(4), 381–389.

Ramanathan, R., Hunt, M. C., English, A. R., Mafi, G. G., & VanOverbeke, D. L. (2019). Effects of aging, modified atmospheric packaging, and display time on metmyoglobin reducing activity and oxygen consumption of high-pH beef. *Meat and Muscle Biology, 3*(1).

Ronkainen, V. P., Skoumal, R., & Tavi, P. (2011). Hypoxia and HIF-1 suppress SERCA2a expression in embryonic cardiac myocytes through two interdependent hypoxia response elements. *Journal of Molecular and Cellular Cardiology, 50*(6), 1008–1016.

Rajagopal, K., & Oommen, G. T. (2015). Myofibril fragmentation index as an immediate postmortem predictor of Buffalo meat tenderness. *Journal of Food Processing and Preservation, 39*(6), 1166–1171.

Shin, D. H., Lin, H., Zheng, H., Kim, K. S., Kim, J. Y., Chun, Y. S., … Kim, S. J. (2014). HIF-1α–mediated upregulation of TASK-2 K+ channels augments Ca2+ signaling in mouse B cells under hypoxia. *The Journal of Immunology, 193*(10), 4924–4933.

Saotome, M., Katoh, H., Satoh, H., Nagasaka, S., Yoshihara, S., Terada, H., & Hayashi, H. (2005). Mitochondrial membrane potential modulates regulation of mitochondrial Ca2+ in rat ventricular myocytes. *American Journal of Physiology-Heart and Circulatory Physiology, 288*(4), H1820–H1828.

Sasabe, E., Tatemoto, Y., Li, D., Yamamoto, T., & Osaki, T. (2005). Mechanism of HIF-1α-dependent suppression of hypoxia-induced apoptosis in squamous cell carcinoma cells. *Cancer Science, 96*(7), 394–402.

Shen, L., Lei, H., Zhang, S., Li, X., Li, M., Jiang, X., … Zhu, L. I. (2014). The comparison of energy metabolism and meat quality among three pig breeds. *Animal Science Journal, 85*(7), 770–779.

Song, S., Ayon, R. J., Yamamura, A., Yamamura, H., Dash, S., Babicheva, A., … Yuan, J. X. J. (2017). Capsaicin-induced Ca2+ signaling is enhanced via upregulated TRPV1 channels in pulmonary artery smooth muscle cells from patients with idiopathic PAH. *American Journal of Physiology-Lung Cellular and Molecular Physiology, 312*(3), L309–L325.

Tadini-Buoninsegni, F., Smeazzetto, S., Gualdani, R., & Moncelli, M. R. (2018). Drug interactions with the Ca2+-ATPase from sarco (endo) plasmic reticulum (SERCA). *Frontiers in Molecular Biosciences, 5*, 36.

Tokumitsu, H., Iwabu, M., Ishikawa, Y., & Kobayashi, R. (2001). Differential regulatory mechanism of Ca2+/calmodulin-dependent protein kinase kinase isoforms. *Biochemistry, 40*(46), 13925–13932.

Vetrovoy, O., & Rybnikova, E. (2019). Neuroprotective action of PHD inhibitors is predominantly HIF-1-independent: An Editorial for 'Sex differences in neonatal mouse brain injury after hypoxia-ischemia and adaptaquin treatment'on page 759. *Journal of Neurochemistry, 150*(6), 645–647.

Wicks, J., Beline, M., Gomez, J. F. M., Luzardo, S., Silva, S. L., & Gerrard, D. (2019). Muscle energy metabolism, growth, and meat quality in beef cattle. *Agriculture, 9*(9), 195.

Winder, W. A., & Hardie, D. G. (1999). AMP-activated protein kinase, a metabolic master switch: Possible roles in type 2 diabetes. *American Journal of Physiology-Endocrinology and Metabolism, 277*(1), E1–E10.

Wang, B., Wood, I. S., & Trayhurn, P. (2008). Hypoxia induces leptin gene expression and secretion in human preadipocytes: Differential effects of hypoxia on adipokine expression by preadipocytes. *Journal of Endocrinology, 198*(1), 127–134.

Williams, A. L., Walton, C. B., MacCannell, K. A., Avelar, A., & Shohet, R. V. (2019). HIF-1 regulation of miR-29c impairs SERCA2 expression and cardiac contractility. *American Journal of Physiology-Heart and Circulatory Physiology, 316*(3), H554–H565.

Wang, L. L., Yu, Q. L., Han, L., Ma, X. L., Song, R. D., Zhao, S. N., & Zhang, W. H. (2018). Study on the effect of reactive oxygen species-mediated oxidative stress on the activation of mitochondrial apoptosis and the tenderness of yak meat. *Food Chemistry, 244*, 394–402.

Wang, L., Ma, G., Zhang, Y., Shi, X., Han, L., Yu, Q., … Ma, J. (2018). Effect of mitochondrial cytochrome c release and its redox state on the mitochondrial-dependent apoptotic cascade reaction and tenderization of yak meat during postmortem aging. *Food Research International, 111*, 488–497.

Xin, K., Hu, B., Han, L., & Yu, Q. (2022). Study on the HIF-1α regulated by glycolytic pathways and mitochondrial function in yaks of different altitudes during postmortem aging. *Journal of Food Biochemistry, e14205*.

Yoshioka, G., Imaeda, N., Ohtani, T., & Hayashi, K. (2005). Effects of cortisol on muscle proteolysis and meat quality in piglets. *Meat Science, 71*(3), 590–593.

Yang, X., Wang, J., Holman, B. W., Liang, R., Chen, X., Luo, X., … Zhang, Y. (2021). Investigation of the physicochemical, bacteriological, and sensory quality of beef steaks held under modified atmosphere packaging and representative of different ultimate pH values. *Meat Science, 174*, Article 108416.

Yang, X., Zhang, Y., Luo, X., Zhang, Y., Zhu, L., Xu, B., … Liang, R. (2022). Influence of oxygen concentration on the fresh and internal cooked color of modified atmosphere packaged dark-cutting beef stored under chilled and superchilled conditions. *Meat Science, 188*, Article 108773.

Zhang, J., Ma, G., Guo, Z., Yu, Q., Han, L., Han, M., & Zhu, Y. (2018). Study on the apoptosis mediated by apoptosis-inducing-factor and influencing factors of bovine muscle during postmortem aging. *Food Chemistry, 266*, 359–367.

Further reading

Wang, L. L., Han, L., Ma, X. L., Yu, Q. L., & Zhao, S. N. (2017). Effect of mitochondrial apoptotic activation through the mitochondrial membrane permeability transition pore on yak meat tenderness during postmortem aging. *Food Chemistry, 234*, 323–331.